

AD-A160 379 STUDY OF LARGE AEROSOL PARTICLES(U) WYOMING UNIV  
LARAMIE DEPT OF PHYSICS AND ASTRONOMY  
D J HOFMANN ET AL. 03 MAY 85 AFGL-TR-85-0096

1/1

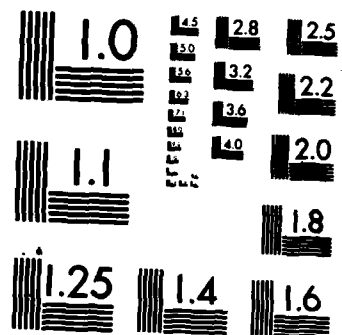
D J HOFMANN ET AL. 03 MAY 85 AFGL-TR-85-0096

D J HOFMANN ET AL. 03 MAY 85 AFGL-TR-85-0096

F19628-82-K-0016

NL

END



MICROCOPY RESOLUTION TEST CHART  
NATIONAL BUREAU OF STANDARDS-1963-A

AFGL-TR-85-0096

# AD-A160 379

12

Study of Large Aerosol Particles

D. J. HOFMANN  
J. M. ROSEN

University of Wyoming  
Department of Physics and Astronomy  
Laramie, Wyoming 82071

3 May 1985

Final Report  
1 December 1981 - 28 February 1984

Approved for public release; distribution unlimited


AIR FORCE GEOPHYSICS LABORATORY  
AIR FORCE SYSTEMS COMMAND  
UNITED STATES AIR FORCE  
HANSOM AIR FORCE BASE, MASSACHUSETTS 01731


DTIC  
ELECTE  
OCT 16 1985  
S B

DTIC FILE COPY

85 10 10 129

This technical report has been reviewed and is approved for publication.

  
FREDERIC E. VOLZ  
Contract Manager

  
ROBERT W. FENN  
Branch Chief

FOR THE COMMANDER

  
JOHN S. GARING  
Division Director

This report has been reviewed by the ESD Public Affairs Office (PA) and is releasable to the National Technical Information Service (NTIS).

Qualified requestors may obtain additional copies from the Defense Technical Information Center. All others should apply to the National Technical Information Service.

If your address has changed, or if you wish to be removed from the mailing list, or if the addressee is no longer employed by your organization, please notify AFGL/DAA, Hanscom AFB, MA 01731. This will assist us in maintaining a current mailing list.

## REPORT DOCUMENTATION PAGE

1a. REPORT SECURITY CLASSIFICATION Unclassified			1b. RESTRICTIVE MARKINGS		
2a. SECURITY CLASSIFICATION AUTHORITY			3. DISTRIBUTION/AVAILABILITY OF REPORT Approved for public release; distribution unlimited		
2b. DECLASSIFICATION/DOWNGRADING SCHEDULE					
4. PERFORMING ORGANIZATION REPORT NUMBER(S)			5. MONITORING ORGANIZATION REPORT NUMBER(S) AFGL-TR-85-0096		
6a. NAME OF PERFORMING ORGANIZATION University of Wyoming		6b. OFFICE SYMBOL (If applicable)	7a. NAME OF MONITORING ORGANIZATION Air Force Geophysics Laboratory		
6c. ADDRESS (City, State and ZIP Code) Dept of Physics and Astronomy Laramie, Wyoming 82071			7b. ADDRESS (City, State and ZIP Code) Hanscom AFB Massachusetts 01731		
8a. NAME OF FUNDING/SPONSORING ORGANIZATION Air Force Geophysics Laboratory		8b. OFFICE SYMBOL (If applicable)	9. PROCUREMENT INSTRUMENT IDENTIFICATION NUMBER F19628-82-K-0016 -		
8c. ADDRESS (City, State and ZIP Code) Hanscom AFB, MA 01731			10. SOURCE OF FUNDING NOS.		
11. TITLE (Include Security Classification) Study of Large Aerosol Particles			PROGRAM ELEMENT NO. 61102F	PROJECT NO. 2310	TASK NO. G1
					WORK UNIT NO. AW
12. PERSONAL AUTHOR(S) Hofmann, D.J., and Rosen, J.M.					
13a. TYPE OF REPORT Final Report		13b. TIME COVERED FROM 1 Dec 81 to 28 Feb 84		14. DATE OF REPORT (Yr., Mo., Day) 85/05/03	
15. PAGE COUNT 38					
16. SUPPLEMENTARY NOTATION					
17. COSATI CODES			18. SUBJECT TERMS (Continue on reverse if necessary and identify by block number)		
FIELD	GROUP	SUB. GR.	Stratosphere; Aerosol Optical Model; Size Distribution; Laser Backscatter; Volcanic Aerosol; Aerosol Mass. 4		
19. ABSTRACT (Continue on reverse if necessary and identify by block number) In this work a stratospheric aerosol optical model is developed which is based on a size distribution determined from direct measurements and additionally constrained to be consistent with large data sets of independently measured macroscopic aerosol properties such as mass and backscatter. The period under study covers background as well as highly disturbed volcanic conditions and an altitude interval ranging from the tropopause to about 30 km. The predictions of the model are used to interpret and intercompare diverse types of stratospheric aerosol measurements. Key words:					
20. DISTRIBUTION/AVAILABILITY OF ABSTRACT UNCLASSIFIED/UNLIMITED <input type="checkbox"/> SAME AS RPT. <input type="checkbox"/> DTIC USERS <input checked="" type="checkbox"/>			21. ABSTRACT SECURITY CLASSIFICATION Unclassified		
22a. NAME OF RESPONSIBLE INDIVIDUAL F.L. Volz			22b. TELEPHONE NUMBER (Include Area Code) (617) 861-3666		22c. OFFICE SYMBOL OPA

## TABLE OF CONTENTS

Introduction	1
Basic Model Development	3
Applications	12
Conclusions	17
References	18

## LIST OF TABLES

1. Parameters for Size Distribution in Figure 1	22
---	----

## FIGURES

1 Size distributions (LNSP Model)	23
2 Sulfate aerosol versus sampling filter	24
3 Lidar backscatter versus measurements	25
4 Same as Figure 3, $\lambda 1.06\mu\text{m}$	26
5 Peak/mixing ratio and average mass radius 1981-1985	27
6 Backscatter/mass ratio versus channel ratio, $\lambda 0.69\mu\text{m}$	28
7 Backscatter/mass ratio versus channel ratio, $\lambda 1.06\mu\text{m}$	29
8 Wavelength dependence of backscatter	30
9 Optical depth/column mass ratio vs channel ratio aerosol	31
10 Optical depth versus wavelength	32
11 Typical scattering phase function	33
12 Asymmetry factor versus channel ratio	34

**DTIC**  
**ELECTE**  
**S** **D**  
**OCT 16 1985**  
**B**



Accession	✓
NTIS	
DTIC	
Aviation	
Aviation	
By	
Distribution	
Aviation	
Dist	
<b>A-1</b>	

## 1. Introduction

An accurate and versatile optical model of stratospheric aerosols has important applications in many areas of geophysical research. Such models are indispensable for the interpretation of both satellite and ground based remote optical sensors that monitor the stratospheric aerosol layer. They can also provide the basis for comparison of rather diverse types of measurements, such as evaluating the consistency between mass and scattering properties. Stratospheric aerosols have been known to adversely affect the operation of remote sensing devices<sup>1</sup> and a good optical model would provide the basis for recognizing and possibly removing the degrading effects. In addition a versatile model should be able to provide reliable estimates of quantities or parameters that have not been measured or that are inconvenient to measure. Finally it might be observed that the overall success of an optical model is a direct measure of the inter-observational consistency and the degree to which the aerosol system itself is understood.

Although a relatively large number of studies have been conducted that deal with stratospheric aerosol scattering properties, only a few efforts have been directed toward a comprehensive model that could be used to make general predictions and form the basis for inter-instrumental comparisons. Shettle and Fenn<sup>2</sup> proposed a gamma size distribution function which they considered appropriate for optical modeling. The variable parameters in this function allow for a large variety of size distribution types. However, their choice of parameters was not necessarily based on direct size distribution measurements in the stratosphere.

Pinnick et al<sup>3</sup> proposed a simple exponential and lognormal size distribution function that was based on a large data base of directly measured submicrometer size aerosol. The model was used to compare particle concentration measurements with observed lidar backscattering. It was also used to estimate the dependence of aerosol extinction and backscatter on wavelength and to calculate the planetary albedo of stratospheric aerosols.

Toon and Pollack<sup>4</sup> proposed a global stratospheric aerosol model based on a zold distribution function, index of refraction and total optical thickness consistent with several studies available at that time. (The zold distribution has been shown to be equivalent to the lognormal distribution<sup>5</sup>.) This model was used in radiative transfer calculations for studies in long term climate effects.

Russell et al<sup>6</sup> made an effort to utilize essentially all of the previously proposed size distributions in one unified approach. The resulting optical model provided the basis for comparing a relatively large number of diverse types of observations made during two extensive field campaigns<sup>7,8</sup>.

More recently Lenoble and Brogniez<sup>9</sup> have employed bimodal size distribution functions in optical model calculations. However, this was a theoretical study and the size distributions themselves were not directly matched to actual measurements.

All of the above optical models that were based on measured size distributions appear to be relatively successful. However, with the possible exception of the work of Lenoble and Brogniez<sup>9</sup> these models were applied to relatively undisturbed conditions in the stratosphere and it was not possible until now to make a real test of their general applicability to a wide variety of natural conditions. As a result of a series of volcanic eruptions beginning with Mt. St. Helens in May 1980 and ending with El Chichon in April 1982, the stratospheric aerosol layer has undergone a very significant change in both concentration and size distribution<sup>10</sup>. The present period (since Jan. 1983) is characterized by a relatively smooth and slow decay of the net disturbance. This stratospheric perturbation, which may not occur again within the next 100 years<sup>10</sup>, has provided an unusual opportunity to further test and advance stratospheric aerosol optical models.



## II. Basic Model Development

### A. Preliminary Considerations

The particle size distribution, shape and composition are usually at the heart of all serious optical models. Fortunately, stratospheric aerosols are very probably essentially spherical and homogeneous due to their liquid nature (approximately 75% solution of sulfuric acid) and therefore Mie scattering theory can be applied with some degree of confidence. Recent studies of the effect of composition and temperature on stratospheric aerosol index of refraction suggest that this component of the optical model is fairly well known and predictable<sup>11</sup>. Using the calculation procedure of Russell and Hamill<sup>11</sup> we have found that for all of our soundings (excluding those made within a few weeks after a volcanic eruption) the index of refraction in the main part of the aerosol layer (15 - 20 km) varies only between about 1.44 and 1.45. A value of 1.45 has been chosen for most of this work since it is a value often used for the visible wavelength region. The sensitivity of the results to the particular choice of index of refraction will be discussed in a later section.

The primary effort in developing the optical model here is therefore directed toward constructing a size distribution that is consistent with a number of well determined independent constraints. The authors' past experience with size distribution measurements indicates that the results obtained from a single method or investigator should never be accepted indiscriminately as a source of this fundamentally important aerosol feature. Optical particle counters, for example, suffer from double valued response in some part of the size spectrum<sup>12,13</sup>. Impactor type devices are frequently used to sample stratospheric aerosols and while they do not have the double valued response problem, some unknown amount of evaporation of the particles may take place before the samples are processed. In addition, there is some uncertainty in relating the distorted shape of the particles on the collecting substrate to the original particle diameter in the

free stratosphere. Size dependent collecting efficiency as a function of altitude must also be taken into account.

In this study we generate a candidate size distribution consistent with our extensive data set derived from a balloon borne system of optical particle counters. Careful consideration has been given to avoiding particle size regions where the counters experience double valued response. The systematic accuracy of the mass and scattering properties predicted by the candidate distribution is then tested against extensive sets of direct measurements made by other independent research groups.

This procedure differs from previous studies in that it involves developing a consistent size distribution from the constraints offered by several extensive data sets covering a wide range of stratospheric aerosol conditions. In this approach we seek to avoid "tuning" the size distribution to a specific stratospheric condition or to the results of a few specific field measurements.

#### B. Experimental Procedure

A balloon borne system of three individual optical particle counters was used in this work to obtain an initial estimate of the size distribution as a function of altitude. One counter was dedicated to measuring the concentration of all particles greater than about 0.01 micrometer diameter, which for the stratosphere can be interpreted as essentially the total aerosol concentration. Details of this instrument ( which operates as a high supersaturation condensation nuclei counter) have been presented elsewhere<sup>14</sup>.

The second optical particle counter consists of our standard two channel dustsonde<sup>15</sup>, which determines the concentration of particles greater than 0.15 and 0.25 micrometers radius. An estimate of the slope of the distribution in this size range is given by the ratio of the counting rates in channel I (radius > 0.15  $\mu\text{m}$  ) and channel II (radius > 0.25  $\mu\text{m}$  ) and will hereafter be referred to as the channel count ratio I/II. This instrument has been in use for more than 20 years and is known to produce results consistent with a wide variety of other types of instrumentation

for background aerosol conditions<sup>7,8,16,17,18,19</sup>. The past success of the dustsonde can be attributed to its relatively accurate sizing capabilities (it has been shown that this counter is not affected by the double valued response region<sup>13</sup>) and to the fact that even though its size range is very limited, it is the size range most relevant to visible light scattering properties for stratospheric aerosol background conditions. As will be demonstrated below however, the standard dustsonde does not necessarily cover an adequate size range for the disturbed stratosphere.

The third optical particle counter used in the compliment of flight instrumentation is a dustsonde modified for high volume sampling and capable of measuring particle concentrations greater than four different radii: 0.25, 0.95, 1.20 and 1.80  $\mu\text{m}$ . The smallest particle channel overlaps with the standard dustsonde measurement and we require agreement between the two instruments for the overall sounding to be considered reliable. The light scattering geometry of the modified dustsonde is essentially identical to that of the standard dustsonde so that the previous instrument response analysis is for the most part still applicable<sup>13</sup>. This analysis shows that the 1.20 and 1.80  $\mu\text{m}$  channels operate well out of the double valued response region while the 0.95  $\mu\text{m}$  channel is very close to it. Considering the fact that for mono-dispersed calibration aerosols, the modified dustsonde displays a somewhat broader pulse height spectrum than the standard dustsonde, a revised response analysis might be in order and could put the 0.95  $\mu\text{m}$  channel in the double valued response region. We believe, however, that the 1.2 and 1.8  $\mu\text{m}$  channels are still outside of the double valued response region. Thus there is reason to exercise a good deal of caution in utilizing the 0.95  $\mu\text{m}$  channel. The analysis given here will proceed along two paths: one in which the information in the potentially suspect channel is retained, and one in which it is ignored. Certainly it is not inappropriate to disregard one channel (only a loss in size distribution structure would result with a corresponding smaller probability of obtaining a useful size

distribution) but rather misleading results may develop by including it. From the beginning it was recognized that there may be some potential problem with the 0.95  $\mu\text{m}$  channel. Our reasoning in choosing the location of the four size channels was as follows: the 0.25  $\mu\text{m}$  size provides a calibration overlap with the standard two channel dustsonde. The 0.95  $\mu\text{m}$  size is the closest value of radius to 0.25  $\mu\text{m}$  that still has a chance of being out of the double valued response region. The 1.20  $\mu\text{m}$  size was considered a backup channel to the 0.95  $\mu\text{m}$  channel in the event this latter channel displayed suspicious results. The fourth channel was chosen for as large a particle size as possible consistent with obtaining a workable counting rate as governed by the sampling flow rate.

#### C. Data Base

The six channel optical particle counter system was first flown in November 1980, (after the disturbance caused by the Mt. St. Helens eruption) but regular soundings did not start until mid 1982. At present about 35 of these types of soundings have been conducted from Laramie. This paper will initially focus on the data obtained after January 1, 1983, because that date marks the beginning of a smooth decay mode in which the stratosphere was relatively well mixed but still of a considerably different character than the background aerosol. We believe that this is an optimal time for comparing data bases generated from the various observational techniques employed at mid-latitude locations.

#### D. Size Distributions

From the above considerations it is seen that there are at most six experimentally determined points available for defining the entire integral size distribution curve and that a rather large gap in information exists between 0.25 and about 1  $\mu\text{m}$  radius. The first step in this modeling effort centers around developing a method for finding a "smooth" curve passing through the experimentally determined data points. By smooth we mean that the first and second derivatives should be continuous. This guarantees

that the differential size distribution as well as its slope is continuous - a seemingly basic requirement for a realistic size distribution. In addition, it will be required that this smooth size distribution satisfy the constraints imposed by other measurements as described below. The reader will recognize that this procedure could lead to many size distributions satisfying the same constraints within the experimental accuracy, but we proceed on the working assumption and expectation that all such distributions will be similar and will produce similar results.

Before directly proceeding with the invention of new size distributions some remarks concerning the adequacy of previously used size distributions might be in order. During relatively undisturbed periods it was found that the two channel standard dustsonde data could be used to define a simple exponential size distribution that would adequately account for the scattering and mass properties of the aerosol<sup>3,7,8</sup>. Some refinement was made to this size distribution model by including a third channel measurement in which the total aerosol concentration was determined with a condensation nuclei counter. With these three channels of information it was possible to define a unique lognormal distribution which was equally satisfactory in explaining the observed aerosol mass and scattering properties but treated the small particle region more realistically<sup>3,7,8</sup>. For future reference these early models were used to calculate the background properties where illustrated in the applicable figures.

The exponential and lognormal size distributions determined from the two or three channel data after the 1982 eruption of El Chichon failed quite badly in that they were not consistent with either the five or six channel size data and were not consistent with the observed aerosol mass and scattering properties. Not surprisingly, the reason for the failure can be attributed to the fact that the two or three channel size data cannot simply be extrapolated to correctly account for the concentration of the larger particles. Even though the early models probably did not accurately treat the large particle size range, they were still successful because the concentrations in this size region were too

small to effectively contribute to the aerosol mass and scattering properties. We are thus forced to consider some new functional forms to describe the perturbed size distribution following the El Chichon eruption.

An exhaustive discussion dealing with the merits and deficiencies of the various size distributions tested in this study would be quite tedious and lengthy. We therefore present only a summary of the reasoning leading to one successful choice.

Some success has been achieved by fitting the six channel size data to a two mode lognormal size distribution<sup>19</sup>. This procedure seems to be relatively satisfactory for the decay period following the Mt. St. Helens eruption, (excluding the observations of the original cloud passing over Laramie) but not for the period following the El Chichon eruption because it generally overestimates the aerosol mass and scattering properties and gives a suspiciously narrow mode near the suspect  $0.95 \mu\text{m}$  radius channel. At first this result seemed plausible because it was consistent with higher resolution size distribution measurements made by other groups during the same time period<sup>20,21</sup>. At present, however, a comparison with the other methods indicates that the concentration implied from the  $0.95 \mu\text{m}$  channel measurement is considerably (over a factor of 10) too large. The explanation for this discrepancy could well be that this particle channel is influenced by the double valued region of the instrument response as discussed above. We have temporarily abandoned efforts to fit a two mode lognormal function to the size distribution but still recognize that the possibility exists for finding a viable means of utilizing this form.

The spline curve under tension is a useful, but brute force, method for passing a smooth curve through unequally spaced data points<sup>23</sup>. By adjusting the tension, the curve changes from a cubic spline to straight line segments between the data points. The fit can be made in either linear or log space for each of the two variables (concentration and radius in this case) which gives a total choice of four possibilities, but only two produce acceptable results. Curve fits to quasi-power law distributions

(as might be encountered in the troposphere) are most successful in log-log space. On the other hand, quasi-lognormal or exponential curves (as past experience indicates might be expected in the stratosphere) are best fit in log concentration - linear radius space.

The size distributions obtained with spline fits under tension utilizing all six dustsonde channels generally give unsatisfactory results by overestimating aerosol mass and scattering effects and by requiring high tensions that distort the distribution curves. This result, along with the above concerns expressed for the integrity of the 0.95  $\mu\text{m}$  channel, has led us to abandon its use until its suspicious behavior can be satisfactorily resolved.

A five point spline fit (neglecting the 0.95  $\mu\text{m}$  channel) was also tested. In this case satisfactory results could be obtained by adjusting the value of the tension. However, it was frequently necessary to use relatively high values of tension so that the differential size distribution did not take on negative values in the larger size region. As a consequence of the high tensions the size distribution became unrealistically distorted in the smaller size ranges. This behavior, coupled with the fact that there was no method of independently selecting the correct value of tension, led us to abandon the approach of using a simple spline fit.

One of the most successful functional fits that we have found is a combination of a lognormal and spline curve. In this case a lognormal curve is uniquely fit to the first three size channels (as was done for the undisturbed stratosphere) and truncated at 0.25  $\mu\text{m}$  radius. A spline curve under tension is then matched to the lognormal curve and utilizes the remaining data points except the 0.95  $\mu\text{m}$  channel. The resulting size distribution has continuous first and second derivatives. This type of curve corrects many of the problems associated with simple spline fit. The lognormal portion of the curve inherently treats the small particle range of the distribution in a more realistic fashion and correctly utilizes the total measured aerosol count. Furthermore, adjusting the tension will not distort or affect the distribution in the small particle range and create unrealistic situations. It

should also be noted that this model preserves much of the functional form that was so successful in describing the undisturbed stratospheric aerosol.

In evaluating this lognormal-spline (LNSP) model, calculations were carried out in both log-log and log concentration - linear radius space. Similar results were achieved in both cases when a tension of approximately 2 was used for the log-log space calculation. The results of the log concentration-linear radius space calculation were essentially independent of tension for values between zero and ten. For higher tension values the distribution curves generally became unacceptably distorted.

Figure 1 illustrates two extreme size distributions at the peak of the stratospheric aerosol layer that were created with the LNSP model in log concentration linear radius space ( the plot is in log - log space however). As can be seen the curves are not very sensitive to the value of tension but do show some suspicious structure for the highest value chosen. Table I gives the functional form and parameters describing the size distributions shown in Figure 1 for low values of tension.

The results of the calculations for the LNSP model that will be illustrated here have been done in log concentration - linear radius space because they are essentially independent of tension and as such are uniquely determined without any adjustable parameters. This would not be the case if the calculation were done in log - log space where the value of the tension can have an appreciable affect on the results, and an independent method of selecting the appropriate tension would need to be available.

#### E. Size Distribution Constraints

Using the LNSP size distribution model and an appropriate value for the index of refraction, the total aerosol mass concentration and backscatter cross section were calculated for .5 km altitude intervals throughout the stratospheric aerosol layer. These results were then compared to the direct measurements (at the appropriate altitude ) as reported by independent observers. Only those independent observations were used for which we were able to



obtain a significant data base covering the smooth and well mixed decay period following the El Chichon eruption.

Figure 2 shows the predicted sulfate mass compared to the actual measured values. The calculations were made for a particle specific gravity of 1.65 which corresponds to approximately a 75% sulfuric acid solution. Each value was computed for an altitude corresponding to the actual measurements. The independent mass values were determined from an aircraft borne filter sampling system flown near Laramie within an average of 10 days from the corresponding balloon sounding<sup>24,25,26</sup>. The data covers an altitude range of 13.7 to 19.8 km and a time period extending from April 1981 to November 1983 when the high altitude mass sampling program was unfortunately suspended. Figure 2 also indicates the degree of uncertainty in the measurements as well as the predicted values. The uncertainty in the calculated values arise from the uncertainty in the dustsonde measurements themselves, which has been discussed elsewhere<sup>7</sup>. Considering the fact that there are no adjustable parameters involved, the agreement between prediction and measurement is quite satisfactory for this period which covers a very large range of stratospheric conditions and a respectable altitude interval. We have therefore judged the LNSP size distribution model as being acceptably consistent with actual mass measurements.

Figure 3 shows the predicted aerosol backscatter properties compared to available lidar measurements made at 0.6943  $\mu\text{m}$  wavelength as reported by the NASA Langley Lidar Group<sup>27</sup>. For reasons relating to availability of referenceable data, comparisons were made only at the point in the layer where the quantity "backscattering ratio -1" was a maximum, which was almost always between 15 and 20 km. The comparison covers the smooth decay time period from January 1983 to January 1985 and each data point corresponds to observations made during the same month. Also shown in Figure 3 is an indication of the uncertainties in the comparison that are traceable to the measurements themselves. The relatively good agreement between measurement and prediction indicates that the LNSP size distribution model is acceptably

consistent with the actual aerosol backscattering properties at  $0.6943\text{ }\mu\text{m}$  wavelength.

Figure 4 illustrates a comparison similar to that shown in Figure 3 but corresponding to a wavelength of  $1.06\text{ }\mu\text{m}$ . The direct lidar backscatter measurements were made in Fukuoka Japan as reported by M.Hirono<sup>27</sup> and cover the same time period as Figure 3. Even though a small systematic difference between measurement and prediction may be indicated in Figure 4, we still consider that the LNSP size distribution model is acceptably consistent with direct measurements within the uncertainties involved. The great distance between observation sites and an important difference in latitude (Fukuoka: $33.6^{\circ}\text{N}$ , Laramie: $41.3^{\circ}\text{N}$ ) makes the significance of the relatively minor discrepancies rather difficult to assess.

In our procedure for developing a useful size distribution, the LNSP model might now be considered acceptable because it satisfies the predetermined constraints. More constraints will be included in this process if and when additional types of data bases become available. As previously noted the LNSP size distribution is not unique but we proceed with the application of this model on the working tentative assumption that it will not produce results significantly different from another model conforming to the same constraints. More work in the future may be needed to test this assumption.

### III. Applications

#### A. Magnitude of Disturbance

Before continuing with strictly optical model calculations, the reader should be aware of the range of conditions and the time period for which this model applies. The peak mass mixing ratio and average mass radius as calculated from the model is shown as a function of time in Figure 5. The figure indicates that a large perturbation in both aerosol mass and size was experienced during the study period. It is useful to note that only after the El Chichon eruption did the particle size change significantly.

Figure 5 also shows the channel ratio  $I/II$  and in the discussions below we will show that this parameter can be indispensable for the interpretation of several types of optical measurements.

#### B. Interpretation of Lidar Measurements

It has been suggested that the lidar backscattering to mass ratio (bks/mass) could be relatively constant for a wide variety of size distributions<sup>28</sup>. The LNSP model provides a basis for testing this potentially simplifying relationship for the wide variety of size distributions encountered during the study period. Figure 6 shows a plot of bks/mass as a function of  $I/II$  at the mixing ratio peak for a wavelength of  $0.6943 \mu\text{m}$ . The dashed lines indicate the range of values obtained throughout the entire stratosphere for all soundings. It is clear that bks/mass is not strictly constant for stratospheric aerosols as hoped but the ratio is restricted to a fairly narrow range. It is also clear that a much better estimate of bks/mass could be made if the channel ratio  $I/II$  were available from dustsonde measurements. Figure 6 provides a useful basis for converting lidar backscatter data to mass loading for all altitudes in the stratosphere.

Figure 7 is similar to Figure 6 but the calculation was performed for a wavelength of  $1.06 \mu\text{m}$  and an index of refraction of 1.44 which is consistent with the longer wavelength. In this case the bks/mass ratio varies within wider limits and it is more important to know the  $I/II$  parameter for converting the backscatter measurement to a mass loading estimate.

The model also provides a basis for comparing the consistency of lidar measurements made at different wavelengths. Figure 8 shows the relation between the calculated backscatter and wavelength for a few soundings covering the range of aerosol conditions. The similarity of the curves suggests that it would be relatively unproductive to attempt to derive much information concerning the size distribution of stratospheric aerosols from a study of lidar backscatter as a function of wavelength.

#### B. Optical Depth

Using an approach similar to that of the previous section, the model can be used to relate ground based solar extinction or optical depth measurements to aerosol mass loading. However in this case the measurements usually include the tropospheric component and as such cannot be directly applied to assessing the stratosphere unless the tropospheric optical depth is known to be relatively unimportant. At present the optical model is useful in estimating the contribution of the stratospheric optical depth to the total optical depth. This type of study will be continued when large data sets of optical depth covering the relevant time period become available.

Figure 9 illustrates the consistency of the ratio of optical depth (above 15 km) to the column mass loading (above 15 km) during the period of this study. It would appear that stratospheric optical depths could be converted to mass loading values fairly accurately for column integrated channel 1/II ratio values greater than about 2.5. For lower values of the 1/II ratio, however, some knowledge of this ratio would still be useful in making the conversion.

The calculated dependence of stratospheric optical depth on wavelength is shown in Figure 10 for several representative periods throughout this study. Unlike the corresponding backscatter calculations, the wavelength dependence of optical depth takes on a completely different character after the El Chichon eruption. Direct observations<sup>29</sup> of the optical depth show very similar results to those illustrated in Figure 10. This change in the relationship between the optical depth and wavelength might be considered a signature of the El Chichon eruption in the stratospheric aerosol layer. Furthermore, these results suggest that it is at least potentially possible to extract some useful size distribution information from measurements of atmospheric extinction of solar radiation at two or more wavelengths. Such studies have already been reported<sup>30</sup> but deal with size distribution types not necessarily characteristic of the full range of stratospheric conditions.

### C. Interpretation of Satellite Based Solar Extinction Measurements

Measurements of the intensity of solar radiation traversing the earth's atmospheric limb from a satellite during spacecraft sunrise and sunset represent an important and useful method for remotely sensing and monitoring the stratospheric aerosol layer<sup>7,8</sup>. An accurate optical model must be available to initially verify the operation of the satellite sensors and data reduction algorithms, and later to relate the satellite measurements to other parameters such as particle concentration, mass, and lidar backscatter. In this application the LNSP model produces results similar to those shown in Figures 9 and 10, but specific applications will not be illustrated here because there is unfortunately no mid-latitude satellite extinction measurements available covering the time of this study.

### D. Scattering Phase Function

The scattering phase function is an important aerosol property in many types of radiation transfer calculations. Figure 11 illustrates the scattering phase function predicted from the LNSP model at the peak of the aerosol layer for a typical sounding after the El Chichon eruption and is very similar to those reported by Volz<sup>31</sup>. Henyey and Greenstein<sup>32</sup> have suggested a useful parameterization of these types of phase functions. The basic form is given by

$$S(\theta) = (1-g^2)/4\pi(1 + g^2 + 2g\cos\theta)^{3/2}$$

where  $S(\theta)$  is the normalized phase function,  $\theta$  is the scattering angle and  $g$  is an adjustable asymmetry parameter. This function has been fit to the model prediction shown in Figure 11 (dashed line) and as can be seen, the agreement is very good in the forward direction but relatively poor in the backward direction. Nevertheless, the Henyey - Greenstein function is often thought of as acceptably representing a working approximation to the actual

phase function. Figure 12 shows the variation of  $g$  in the maximum of the aerosol layer during the study period as calculated from the model. As shown the value of  $g$  does not remain strictly constant but a relatively accurate value could be estimated from a knowledge of the channel ratio  $I/I_1$ .

#### E. Lidar Backscatter at $10.6 \mu\text{m}$

The magnitude of aerosol backscatter near  $10 \mu\text{m}$  wavelength is of critical importance in evaluating the feasibility and design of the WINDSAT global wind monitoring system<sup>33</sup>. Developing a global climatology of this parameter from direct measurements would be expensive and time consuming to such an extent that it may well be more cost effective to estimate the backscatter from other types of already available measurements through the use of an acceptable optical model. In applying the LNSP model to such an approach, comparisons of the type illustrated in Figures 2 and 3 should first be made to validate the model for this wavelength region and test the consistency of the observations themselves. Although the data exists for this comparison<sup>34</sup> the study has not yet been successfully completed, but it will eventually offer another important constraint for atmospheric optical models.

#### F. Sensitivity of Scattering properties to Index of Refraction

The LNSP model has been used to estimate the sensitivity of aerosol extinction and backscatter to variations or uncertainties in index of refraction for the range of size distributions encountered during this study period. It was found that for indexes of refraction near 1.45 and  $0.7 \mu\text{m}$  wavelength the extinction decreased between 0 and 4% for a change of  $-0.01$  in the index of refraction. For the same conditions the backscatter decreased by 5 to 12%. As previously discussed the range of indexes of refraction as calculated from our flight data using the model of Russell and Hamill<sup>11</sup> is about 1.44 to about 1.45. The extinction and optical depth measurements are therefore not very sensitive to inadvertent fluctuations in the index of refraction.

#### IV. Conclusion

It would appear that it is possible to develop a relatively satisfactory optical model of stratospheric aerosols from a rather low resolution size distribution measurement supplemented with key constraints derived from other measurements. The specific model employed here is not unique and further work should be done to test the sensitivity of the results to other models satisfying the same constraints. A more satisfactory functional form for the size distribution should be found so that the model itself could more easily be communicated to the end users. At present our entire data base must be accessed to make calculations covering the range of stratospheric conditions.

This work was primarily supported by the Air Force Geophysics Laboratory, Hanscom Air Force Base, Bedford, Mass. Additional support was received from NSF and NASA. We are indebted to E.J. Mroz for allowing us to use his unpublished data.

## References

1. C.A.Barth, R.W.Sanders, R.J.Thomas, G.E.Thomas,B.M.Jakosky and R.A.West,"Formation of the El Chichon Aerosol Cloud",Geophys. Res. Lett.,10, 993-996,(1983).
2. Shettle,E.P.,and R.W.Fenn, "Models of the Atmospheric Aerosols and their Optical Properties",AGARD Conference Proceedings No.183, Optical Propagation in the Atmosphere, AGARD-CP-183, NTIS, AD A028-615, (1975).
3. R.G.Pinnick, J.M.Rosen and D.J.Hofmann,"Stratospheric Aerosol Measurements", III: Optical Model Calculations, J.Atmos.Sci., 33, 304-314, (1976).
4. O.B.Toon,and J.B.Pollack,"A Global Average Model of Atmospheric Aerosols for Radiative Transfer Calculations", J.Appl.Meteor.,15, 225-246, (1976).
5. W.D.Ross,"Logarithmic Distribution Functions for Particle Size", J.Colloid and Interface Sci.,67, 181-182, (1978).
6. P.B.Russell,T.J.Swissler,M.P.McCormick,W.P.Chu,J.M.Livingston and T.J.Pepin,"Satellite and Correlative Measurements of the Stratospheric Aerosol. I: An Optical Model for Data Conversions", J.Atmos.Sci.,38, 1279-1294, (1981).
7. P.B.Russell,M.P.McCormick,T.J.Swissler,W.P.Chu,J.M.Livingston,W.H.Fuller,J.M.Rosen,D.J.Hofmann,L.R.McMaster, D.C.Woods and T.J.Pepin,"Satellite and Correlative Measurements of the Stratospheric Aerosols. II: Comparison of Measurements made by SAM II, Dustsondes and AirBorne Lidar", J.Atmos. Sci.,38,1295-1302, (1981).
8. P.B.Russell,M.P.McCormick,T.J.Swissler,J.M.Rosen,D.J.Hofmann, L.R.McMaster,"Satellite and Correlative Measurements of the Stratospheric Aerosol. III: Comparison of Measurements by SAM II, SAGE, Dustsondes, Filters, Impactors and Lidar",J.Atmos. Sci.,41, 1791-1800, (1984).



9. J.Lenoble and C.Brogniez,"Information on Stratospheric Aerosol Characteristics Contained in the SAGE Satellite Multiwavelength Extinction Measurements", Appl. Opt.,24, 1054-1063, (1985).
10. J.B.Pollack,O.B.Toon,E.F.Danielsen,D.J.Hofmann and J.M. Rosen,"The El Chichon Volcanic Cloud: An Introduction", Geophy. Res. Lett.,10, 989-992, (1983).
11. P.B.Russell and P.Hamill, "Spatial Variation of Stratospheric Aerosol Acidity and Model Refractive Index: Implications of Recent Results", J. Atmos. Sci.,41, 1781-1790, (1984).
12. R.G.Pinnick, and J.J.Auvermann,"Response Characteristics of Knollenberg Light-Scattering Aerosol Counters", J. Aerosol Sci.,10, 55-74, (1979).
13. R.G.Pinnick and D.J.Hofmann,"Efficiency of Light-Scattering Aerosol Particle Counters", Appl. Opts.,12, 2593-2597, (1973).
14. J.M.Rosen and D.J.Hofmann,"Unusual Behavior in the Condensation Nuclei Concentration at 30 km", J. Geophys.Res., 88, 3725-3731, (1983).
15. D.J.Hofmann, J.M.Rosen, T.J.Pepin and R.G.Pinnick, "Stratospheric Aerosol Measurements I: Time Variations at Northern Midlatitudes", J. Atmos. Sci.,32, 1446-1456, (1975).
16. G.B.Northam, J.M.Rosen, S.H.Melfi, T.J.Pepin, M.P.McCormick, D.J.Hofmann and W.H.Fuller,Jr., "A Comparison of Dustsonde and Lidar Measurements of Stratospheric Aerosols", Appl. Opts.,13, 2416-2421, (1974).
17. T.J.Swissler, P.Hamill, M.Osborn, P.B.Russell and M.P. McCormick,"A Comparison of Lidar and Balloon-Borne Particle Counter Measurements of the Stratospheric Aerosol 1974-1980", J. Atmos. Sci.,39, 909-916, (1982).
18. J.M.Rosen and D.J.Hofmann,"Results of Instrument Comparisons for the July 1981 ACE Mission"Univ. Wyoming Atmos. Phys. Report No. AP-69, (1981).

19. D.J.Hofmann, J.M.Rosen, R.Reiter and H.Jager, "Lidar and Balloon-borne Particle counter Comparisons Following Recent Volcanic Eruptions", J. Geophys. Res. 88, 3777-3782, (1983).
20. R.G.Knollenberg and D.Huffmann, "Measurements of the Aerosol Size Distributions in the El Chichon Cloud", Geophys. Res. Lett., 10, 1025-1028, (1983).
21. V.R.Oberbeck, E.F.Danielsen, K.G.Snetsinger, G.V.Ferry, W. Fong and D.M.Hayes, "Effect of the Eruption of El Chichon on Stratospheric Aerosol Size and Composition", Geophys. Res. Lett., 10, 1021-1024, (1983).
22. K.G.Snetsinger, Personal Communication, (1985).
23. A.K.Cline, "Scalar- and Planar- valued Curve Fitting Using Splines Under Tension", Comm. Assoc. Comp. Mach., 17, 218-223, (1974).
24. W.A.Sedlacek, E.J.Mroz, A.C.Lazrus and B.W.Gandrud, "Decade of Stratospheric Sulfate Measurements Compared with Volcanic Activity", J. Geophys. Res., 88, 3741-3776, (1983).
25. E.J.Mroz, A.S.Mason and W.A.Sedlacek, "Stratospheric Sulfate from El Chichon and the Mystery Volcano", Geophys. Res. Lett., 10, 873-876, (1983).
26. E.J.Mroz and W.A.Sedlacek, Recent Data from the High Sampling Program, personal communication, (1985).
27. L.McClelland, J.Crampton and E.Nielsen, Eds., Scientific Event Alert Network Bulletin, 8 - 10, (1983-1985).
28. R.G.Pinnick, S.G.Jennings and P.Chylek, "Relationships Between Extinction, Absorption, Backscattering, and Mass Content of Sulfuric Acid Aerosols", J. Geophys. Res., 85, 4059-4066, (1980).
29. J.J.DeLuisi, E.G.Dutton, K.L.Coulson, T.E.DeFoor and B.G. Mendonca, "On Some Radiative Features of the El Chichon Volcanic Stratospheric Dust Cloud and a Cloud of Unknown Origin at Mauna Loa", J.Geophys. Res., 88, 6769-6772, (1983).

30. G.K.Yue and A.Deepak,"Retrieval of Stratospheric Aerosol Size Distribution from Atmospheric Extinction of Solar Radiation at Two Wavelengths", Appl. Opts. 22, 1639-1645, (1983).
31. Volz, F.E., "Volcanic Turbidity, Skylight Scattering Functions, Sky Polarization and Twilights in New England during 1983, Appl. Optics, 23, 2589-2593, (1984).
32. L.G.Henyey and J.L.Greenstein, "Diffuse Radiation in the Galaxy", Astrophysics J., 93, 70-83, (1941).
33. R.M.Huffaker, Ed., "Feasibility Study of Satellite-Borne Wind Monitoring System, NOAA Tech. Memo. ERR WPL-37, (1978)
34. M.J.Post, "Lidar Observations of the El Chichon Cloud at  $\lambda = 10.6 \mu\text{m}$ ", Geophys. Res. Lett. 10, 846-849, (1984).

TABLE I  
PARAMETERS FOR  
SIZE DISTRIBUTION  
IN FIGURE 1

$$n(r) = N_0(r \sqrt{2\pi} \ln \sigma_g)^{-1} \exp[-.5 \ln(r/r_g)^2 / (\ln \sigma_g)^2] \quad r < .25^*$$

$$N(r) = \exp[ a + br + cr^2 + dr^3 ] \quad r > .25^*$$

Radius Range $\mu\text{m}$	Size Distribution Parameter Type	Parameter Value For	
		18 July 81	12 Feb. 83
0-.25	$N_0$	54.66	10.7
	$r_g$	.071	.214
	$\sigma_g$	1.77	3.13
.25-1.2	a	5.215603	2.145304
	b	-26.254624	-1.354558
	c	18.345978	-4.095808
	d	-5.193810	.613355
1.2-1.8	a	-2.061941	19.878082
	b	-8.030920	-45.234379
	c	3.057170	32.234379
	d	-.903952	-9.339334

\*  $N(r)$  is the integral size distribution.  
 $n(r)$  is the differential size distribution.

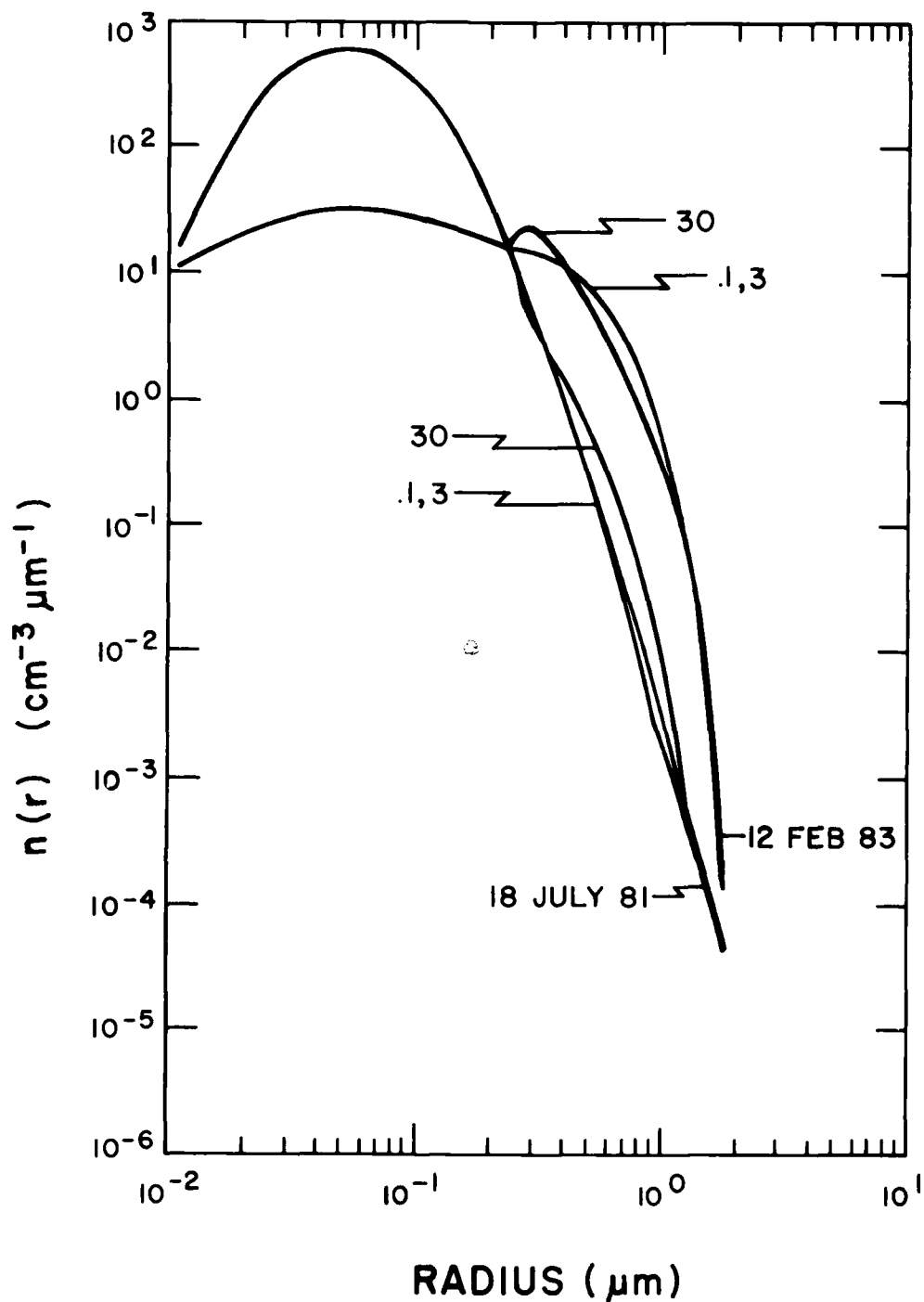


Figure 1. The LNSP model size distribution for two extreme conditions at the peak of the stratospheric aerosol layer. Each curve was constructed for tensions of .1, 3 and 30 as marked. Note that there is very little difference between tensions .1 and 3, but at a tension value of 30 the curve has developed more structure than might be considered consistent with the number of data points defining the curve.

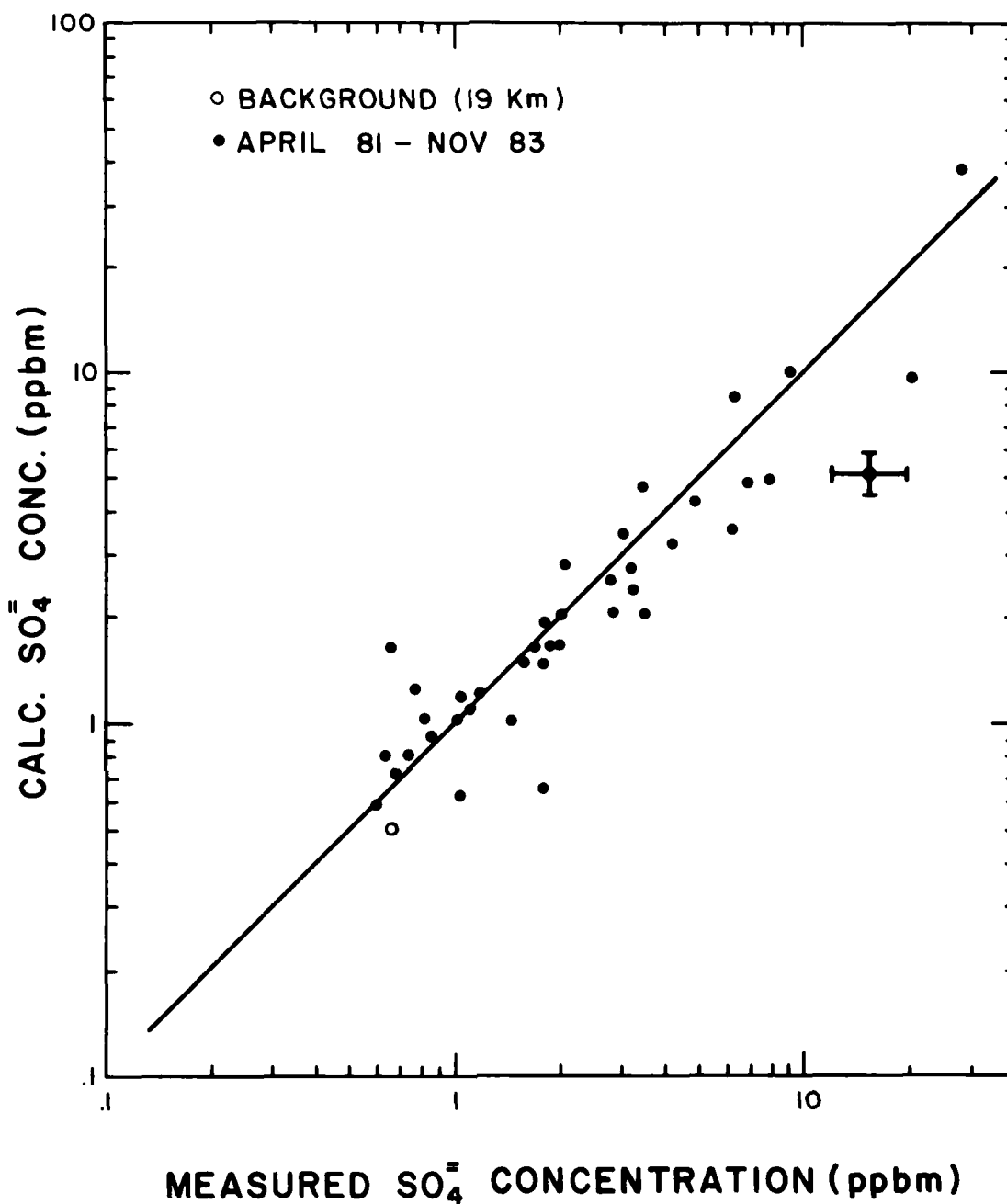


Figure 2. A comparison of the LNSP model predicted sulfate aerosol mass concentration with the measured values derived from aircraft borne filter sampling. The magnitude of uncertainties associated with the comparison is shown for one point only but is typical of all points. The data covers the time period from April 1981 to November 1983 and corresponds to discrete altitudes ranging from 13.7 to 19.8 km.

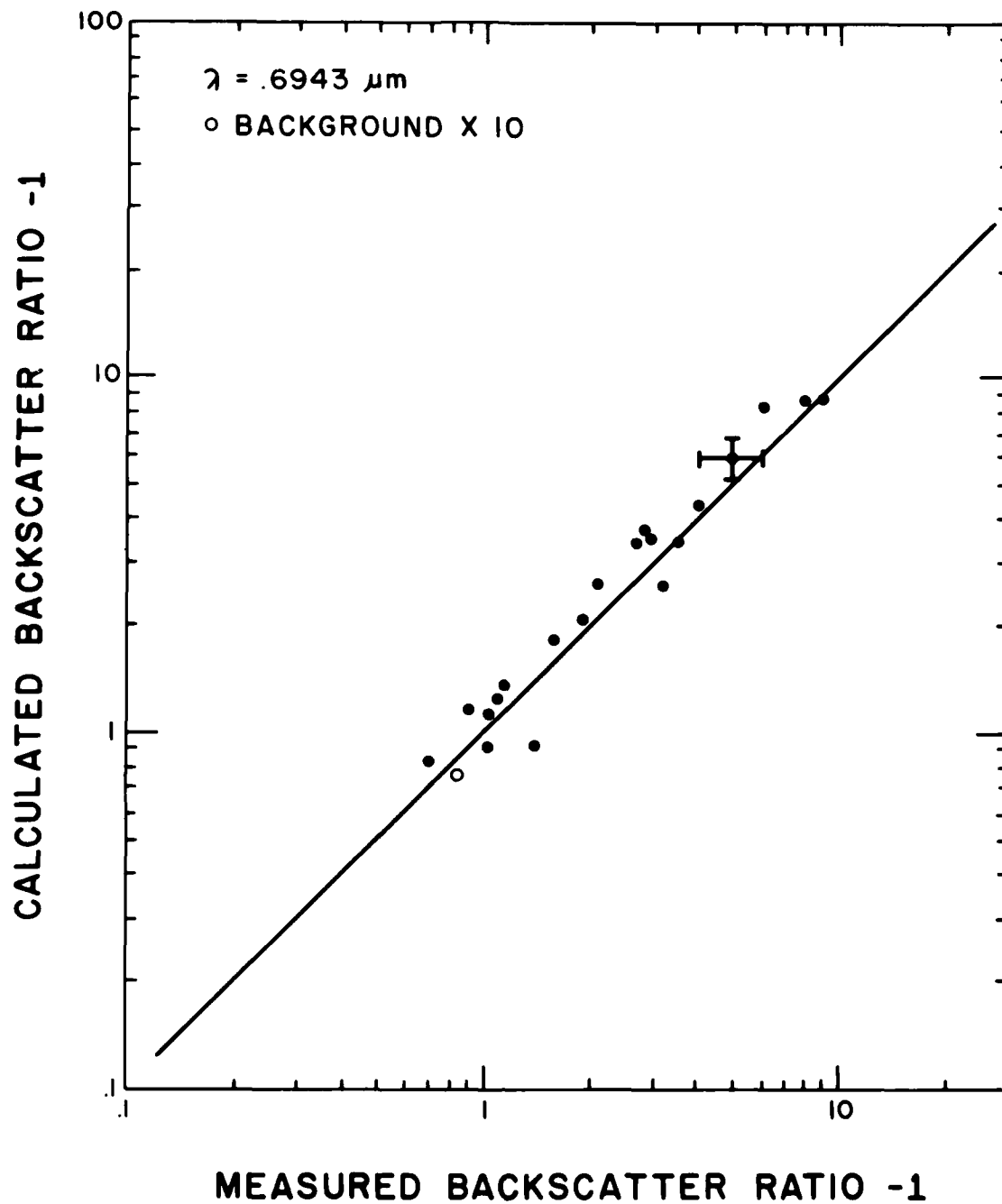


Figure 3. A comparison of the LNSP model predicted lidar backscatter at  $0.6943 \mu\text{m}$  wavelength with actual measurements. The magnitude of the uncertainties associated with the comparison is shown for one point only but is typical of all points. The data covers the time period from January 1983 to early 1985 and corresponds to the peak in the mixing ratio of the stratospheric aerosol layer.

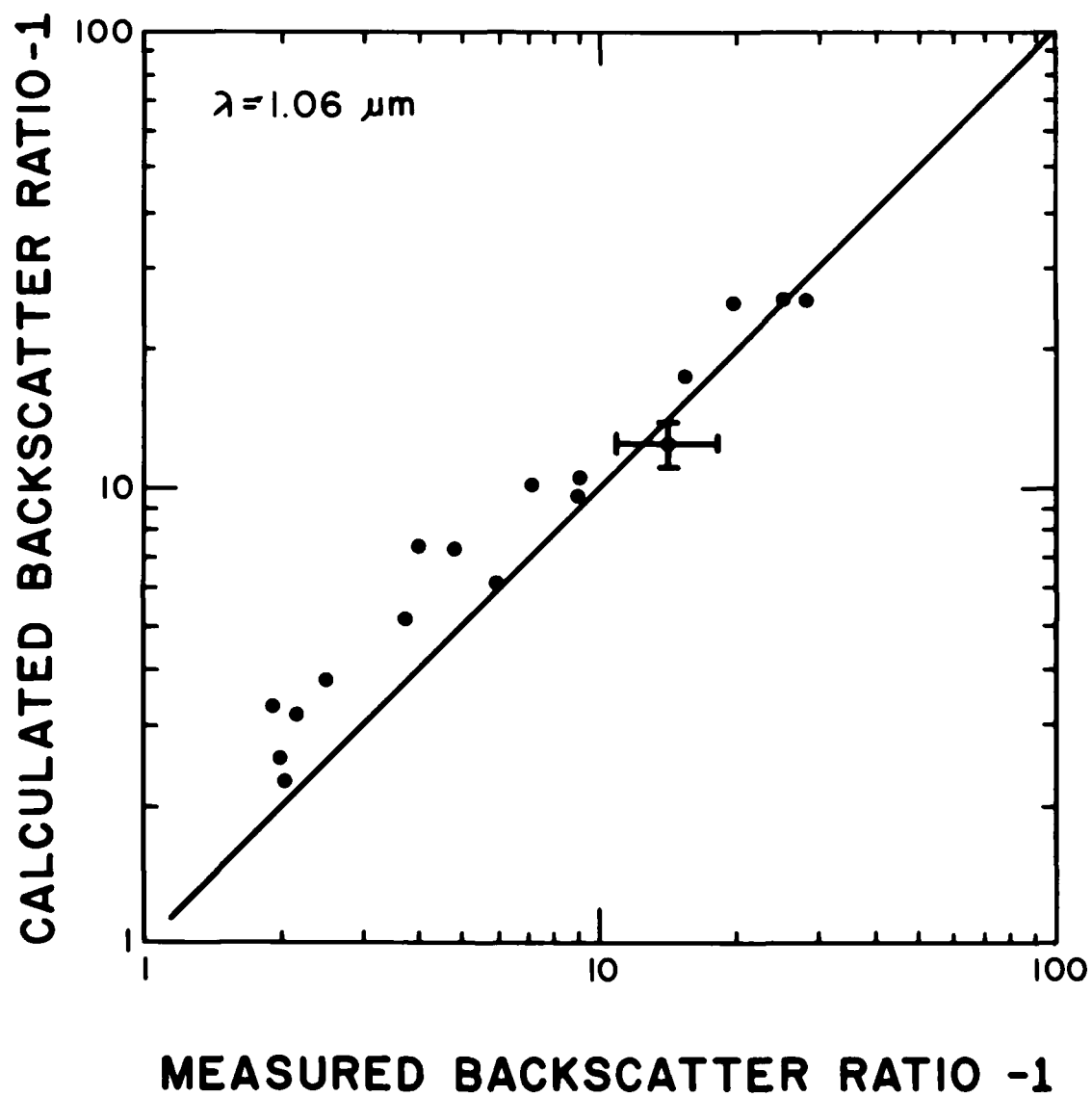


Figure 4. Same as Figure 3, except for a wavelength of 1.06  $\mu\text{m}$



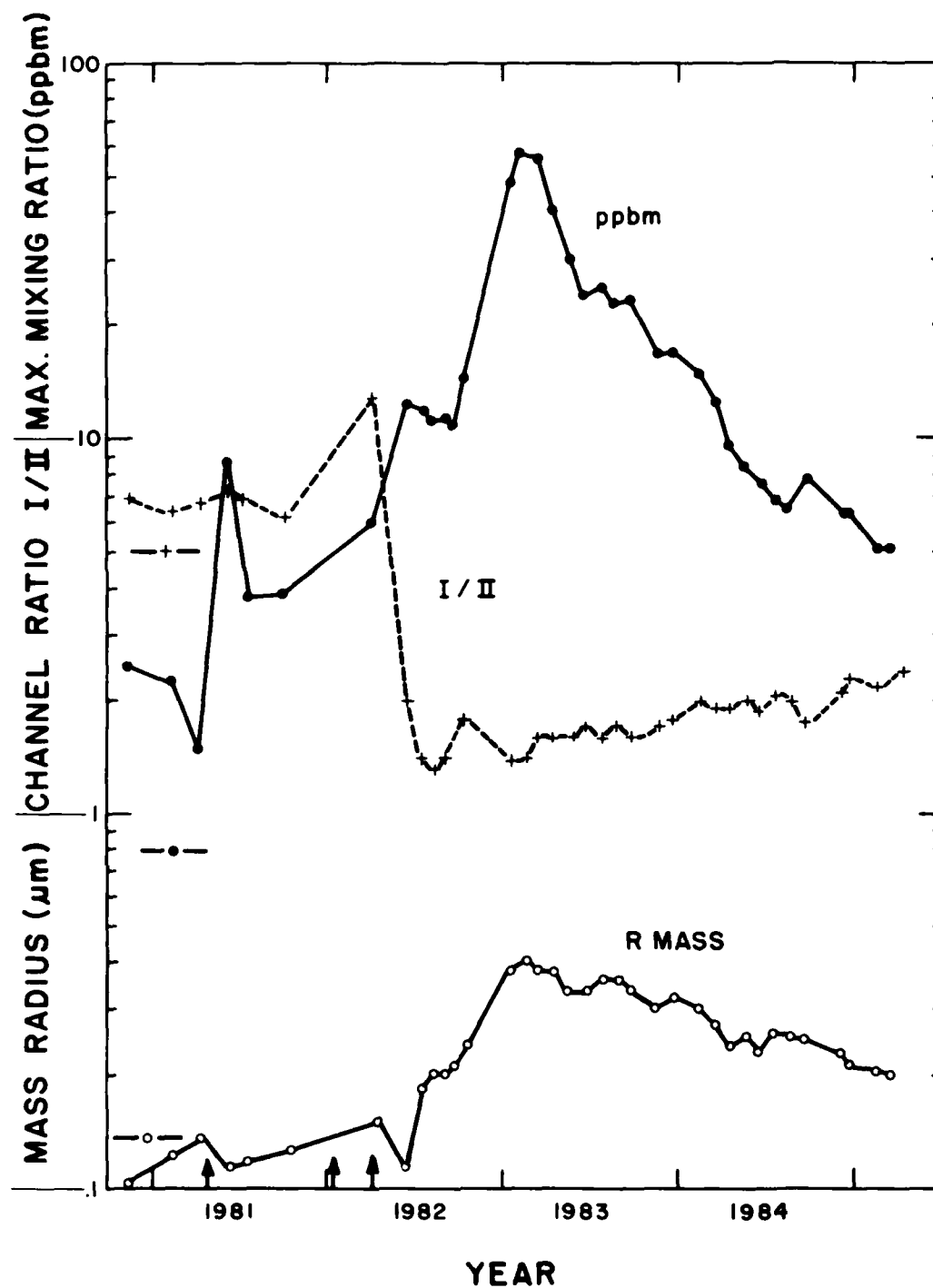


Figure 5. The time development of the peak mixing ratio (ppbm) and average mass radius of the particles in the stratospheric aerosol layer during the study period as predicted by the LNSP model. The horizontal identifying lines at the left indicate background values. The arrows at the bottom indicate major volcanic eruptions.

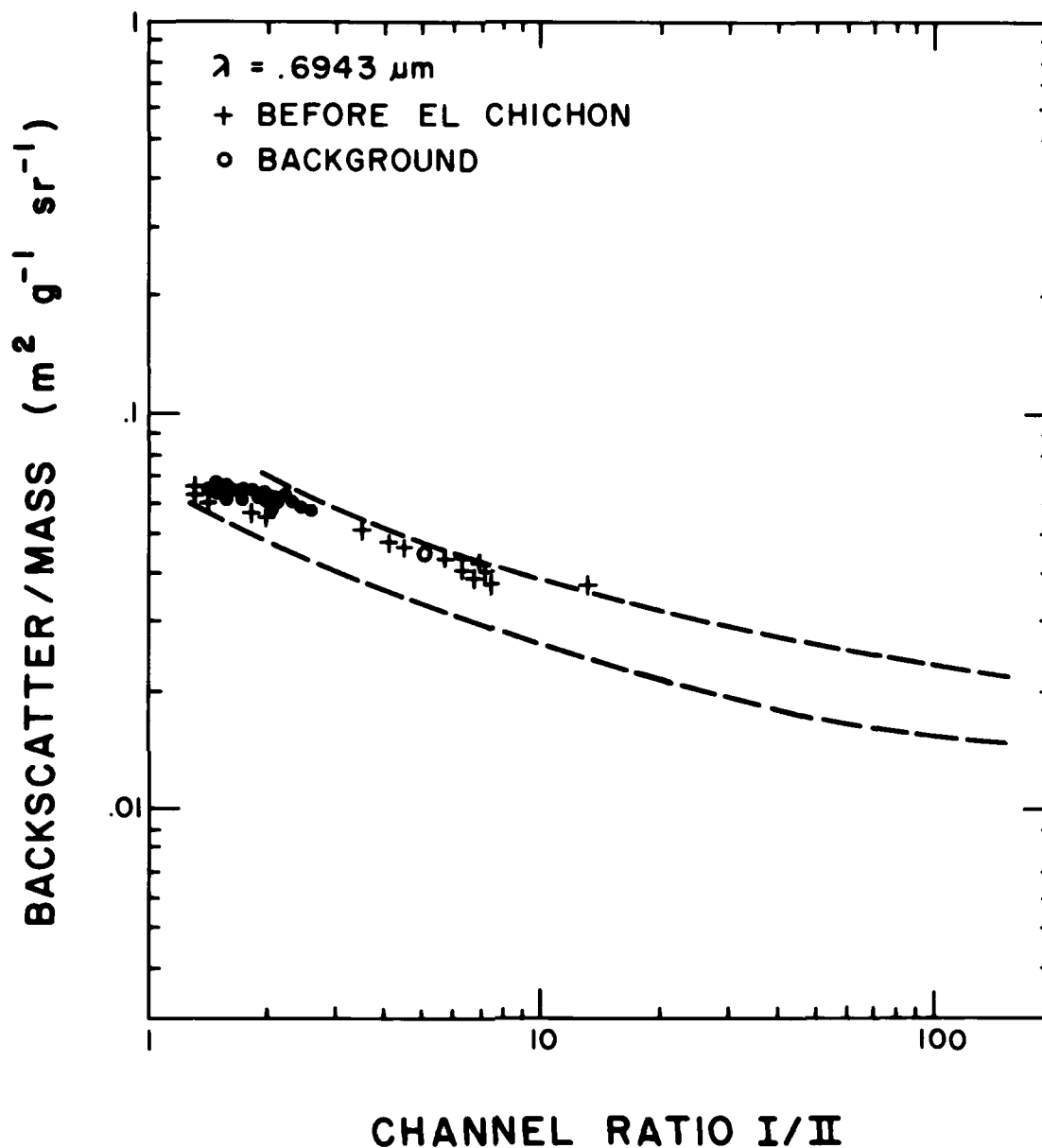


Figure 6. The predicted dependence of the backscatter to mass ratio on the channel ratio according to the LNSP model. The individual points correspond to the peak of the stratospheric aerosol mixing ratio, while the dash lines indicate the range of values for all stratospheric altitudes up to about 30 km. The uncertainties in each point due to uncertainties relating back to the measurement itself is insignificant on the scale of the drawing.

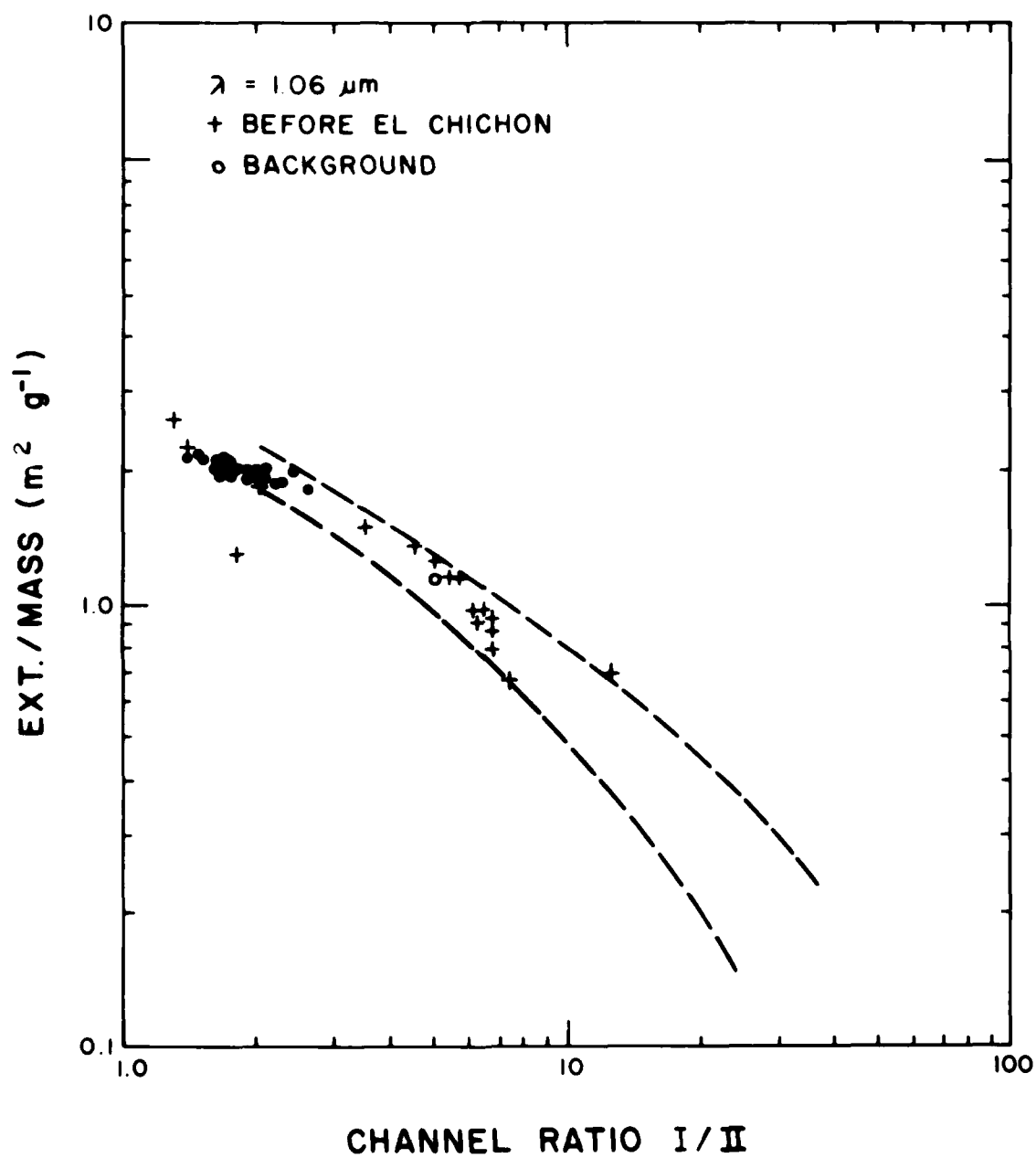


Figure 7. Same as Figure 6, except here the model results deal with the extinction to mass ratio at  $1.06 \mu\text{m}$  wavelength.

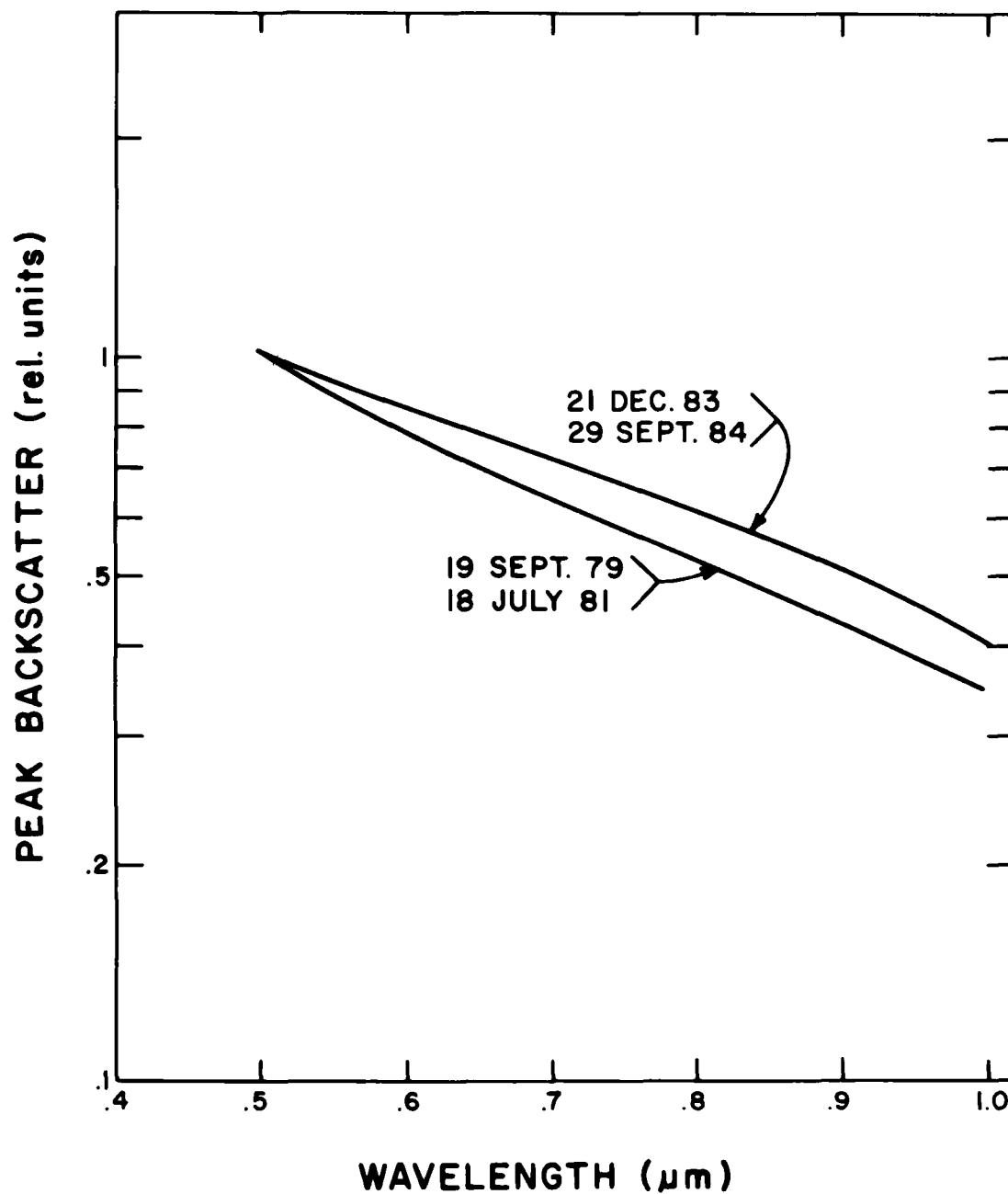


Figure 8. The LNSP model predicted wavelength dependence of the backscatter at the peak of the stratospheric aerosol layer for four soundings covering the range of conditions observed during the study period.

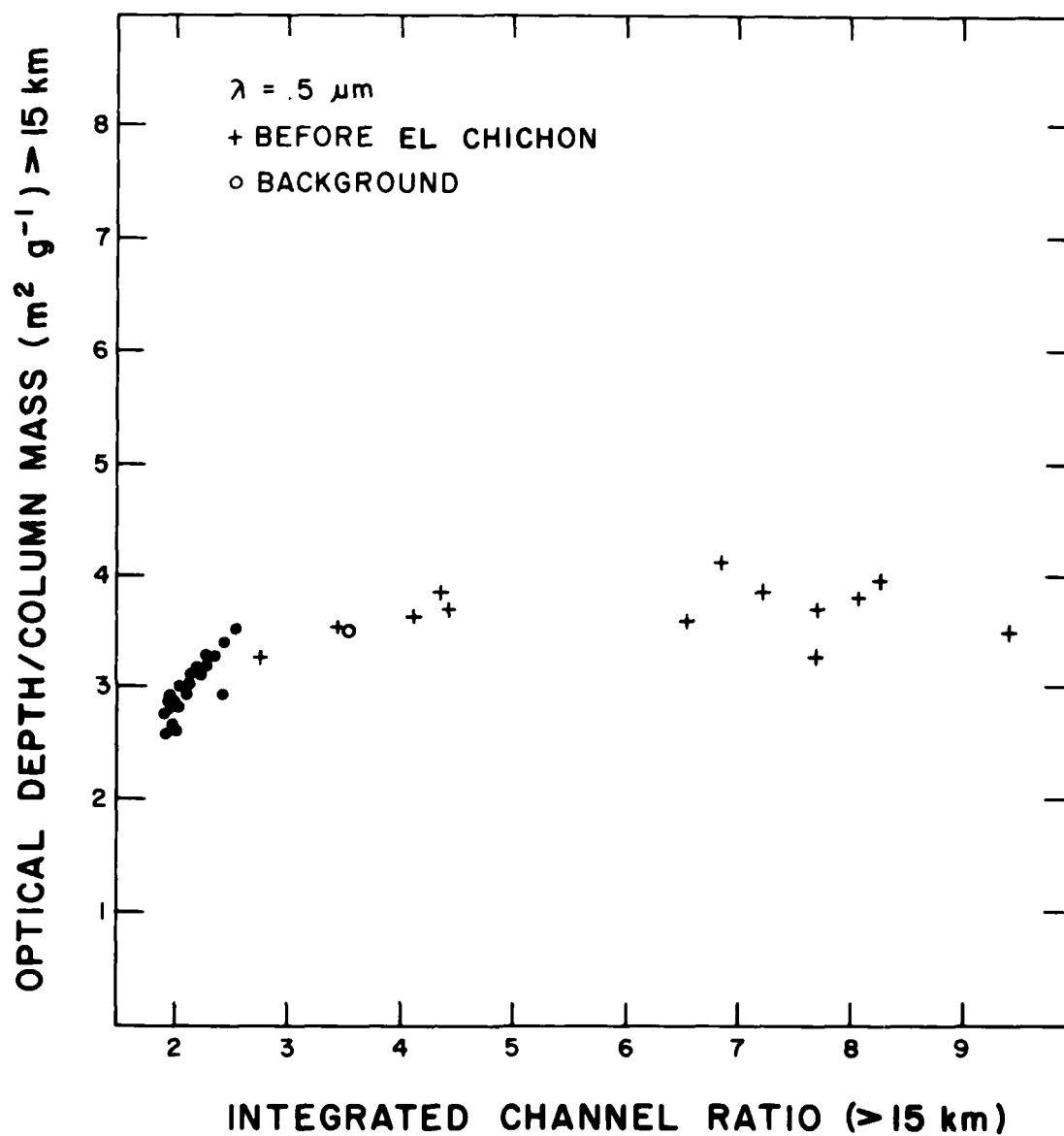


Figure 9. Variability of the optical depth /column mass ratio as predicted from the LNSP model. The integrated channel ratio is the ratio of the column aerosol concentration (above 15 km) in channel I ( $r > 0.15 \mu\text{m}$ ) to that in channel II ( $r > 0.25 \mu\text{m}$ ).

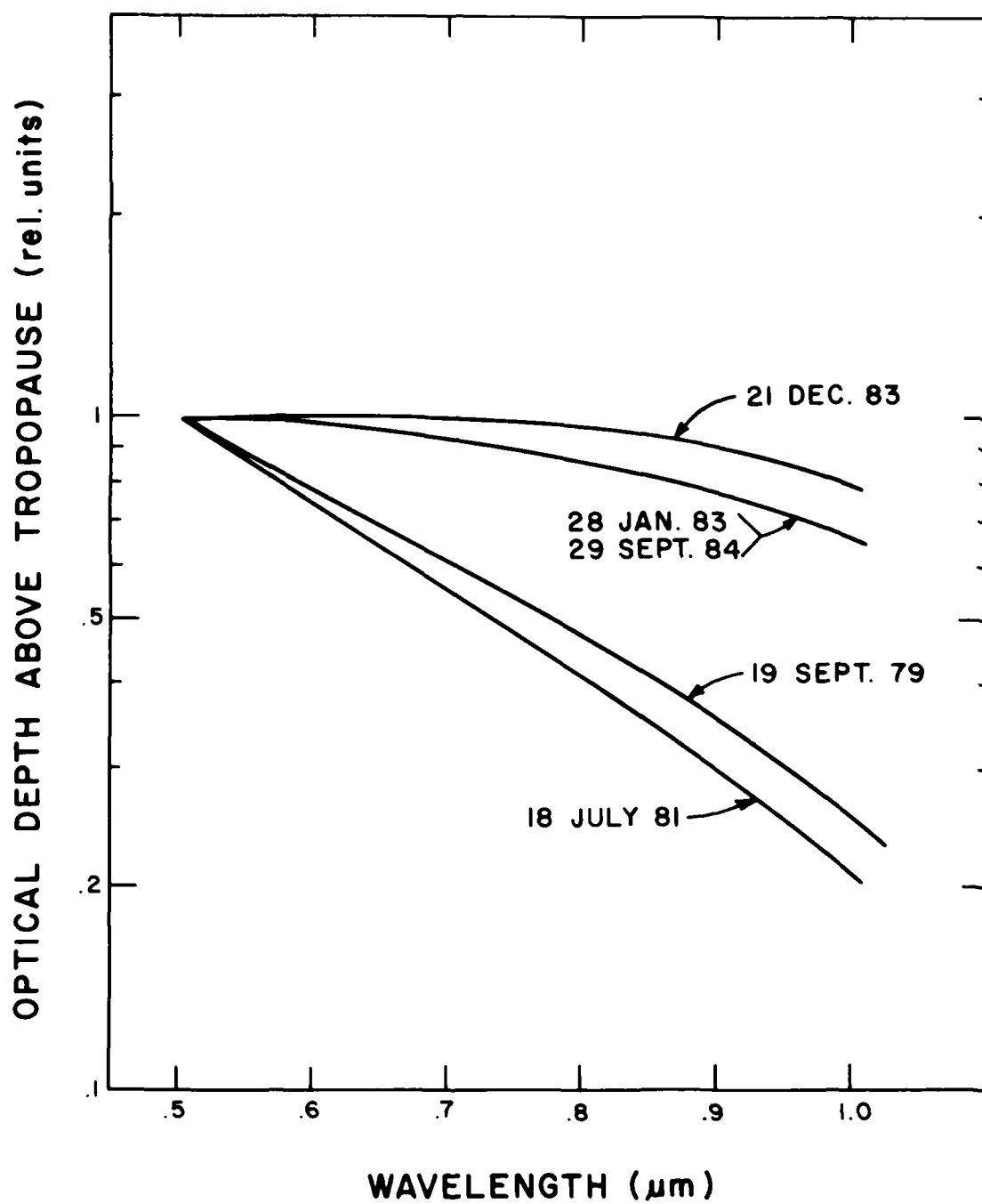


Figure 10. The LNSP model predicted wavelength dependence of optical depth above the tropopause.

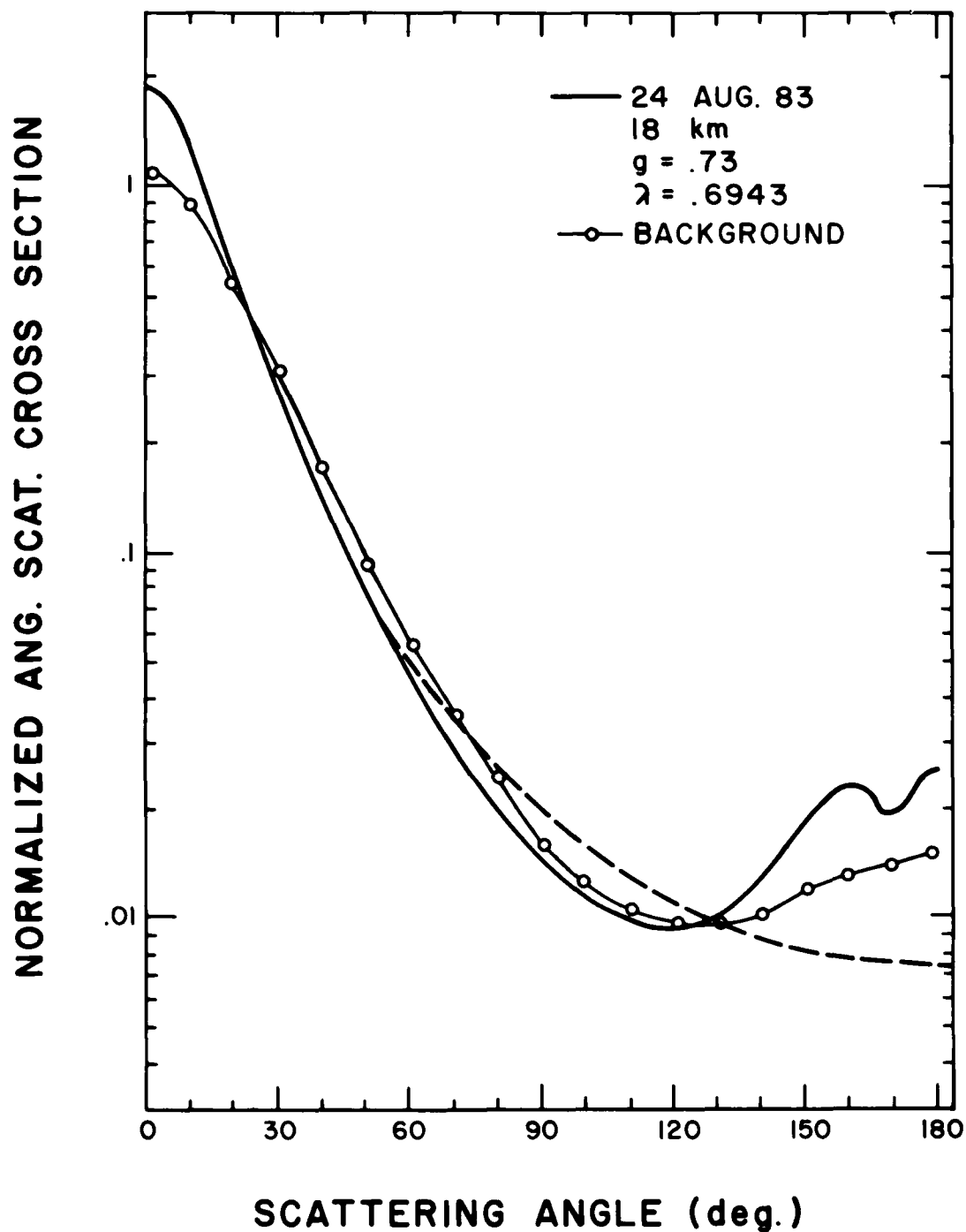


Figure 11. A typical scattering phase function at the peak of the aerosol layer after the El Chichon eruption as calculated from the LNSP model. The dash line represents the Henyey-Greenstein phase function fit to the model results. The value of the asymmetry parameter  $g$  is .73 in this case.

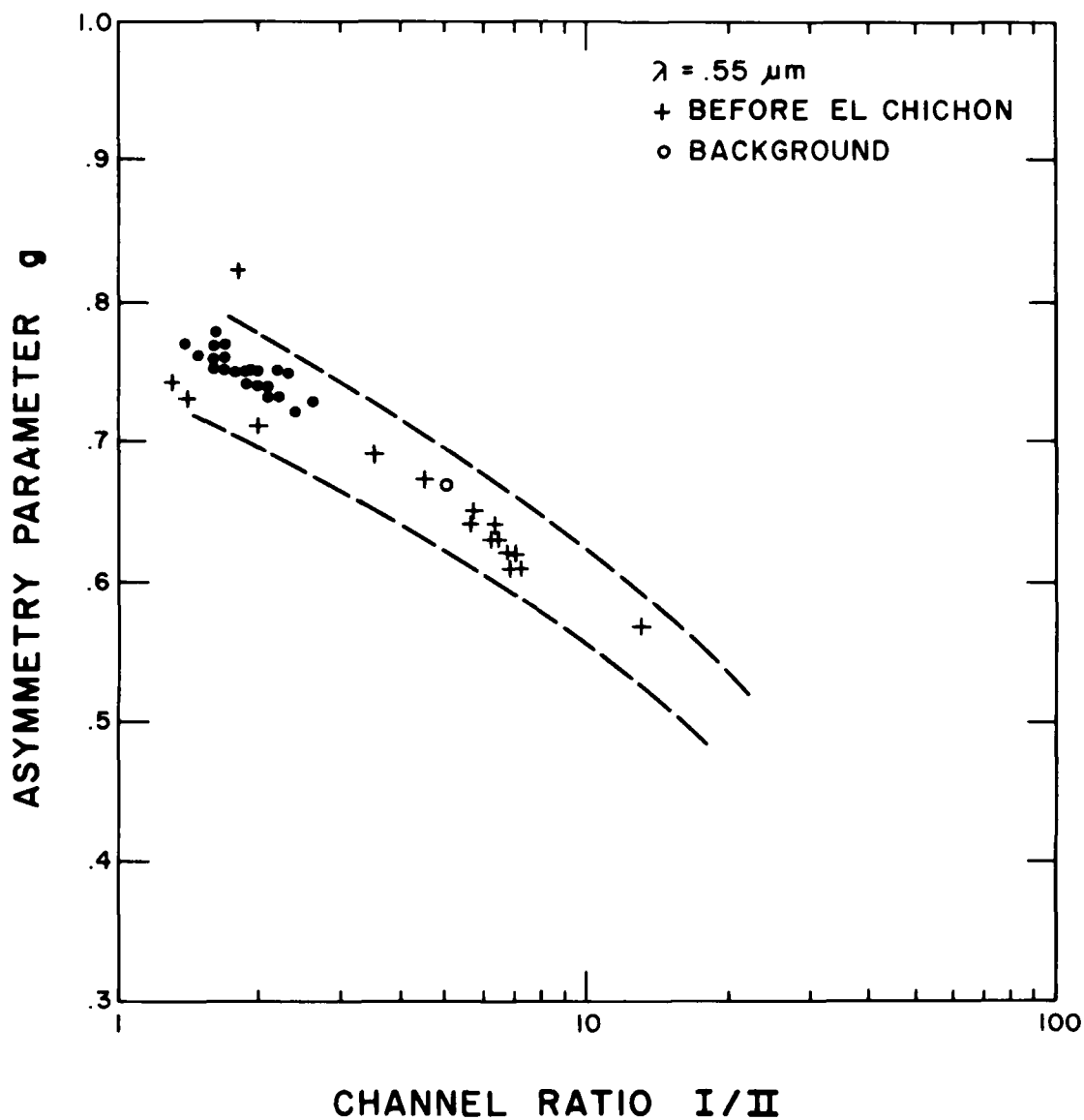


Figure 12. The LNSP model predicted dependence of the Henyey-Greenstein asymmetry factor  $g$  on the channel ratio  $I/II$ . The individual points were derived at the peak of the stratospheric aerosol layer, and the dash lines indicate the range of values obtained throughout the stratosphere.



**END**

**FILMED**

**11-85**

**DTIC**